



ELSEVIER

Surface Science 344 (1995) L1239–L1244

surface science

Surface Science Letters

## Helium scattering from O on Rh(111): scattering cross sections and adsorption kinetics

Kevin A. Peterlinz<sup>1</sup>, S.J. Sibener<sup>\*</sup>

*The James Franck Institute and Department of Chemistry, The University of Chicago, 5640 South Ellis Avenue, Chicago, IL 60637, USA*

Received 18 August 1995; accepted for publication 13 October 1995

### Abstract

He diffraction and specular He scattering measurements of O on Rh(111) were made for  $T_s = 125$ – $625$  K and  $\theta_O = 0.0$ – $0.50$  ML. For  $T_s > 450$  K and  $\theta_O < 0.21$  ML, specular He scattering from the O/Rh(111) overlayer is well described by a model for disordered adsorbates, with a cross section of  $62.6 \text{ \AA}^2$  for 63 meV He. At higher coverages, these measurements reveal a complex relationship between coverage, temperature, and the ordered overlayer structures for O/Rh(111). In addition, adsorption isotherms presented here show second order Langmuir adsorption kinetics for O<sub>2</sub> on Rh(111) and a sticking coefficient of about 5% for O<sub>2</sub> on 525 K Rh(111).

**Keywords:** Adsorption isotherms; Adsorption kinetics; Atom–solid interactions; Atom–solid scattering and diffraction – elastic; Chemisorption; Rhodium

### 1. Introduction

The adsorption of oxygen on noble metal surfaces has been studied extensively in the past in order to understand the origins of the catalytic activity of these metal surfaces in many chemical processes, including reactions in automotive catalytic converters. Generally these studies are limited to either studies of ordered structures at lower temperatures ( $< 300$  K) at which reaction rates are too slow to study catalytic activity, or to studies of kinetics at

higher temperatures ( $> 450$  K for CO oxidation [1–9]) at which ordered structures are either inferred from kinetic models or assumed to be nonexistent.

Recent work from our lab [10] and others [11] has demonstrated the utility of helium scattering in measuring the coverages and ordered phases of adsorbates on low index single crystal metal surfaces. Large cross sections for specular helium attenuation as a function of coverage arise primarily from adsorbate induced modification of the attractive part of the He–surface interaction potential [11]. This local potential modification enhances diffuse scattering, and leads to the associated drop in specular intensity. We present here helium diffraction and specular helium scattering measurements of the O/Rh(111) system for oxygen coverages ( $\theta_O$ ) = 0–0.50 ML (mono-

<sup>\*</sup> Corresponding author. Fax: +1 312 702 5863; E-mail: sibener@silly.uchicago.edu.

<sup>1</sup> Present address: Chemistry Department, George Washington University, 725 21st Street, N.W., Washington, DC 20052, USA.

layers) and  $T_s$  (surface temperature) = 125–650 K, well within the range of temperatures for which Rh is catalytically active. These measurements revealed a complex but consistent relationship between  $\theta_0$  and helium reflectivity that, like our previous measurements for CO/Rh(111) [10], allow us to calibrate and measure  $\theta_0$  via specular He scattering over a wide range of temperatures. In addition, analysis of the diffraction and specular He scattering measurements allowed us to determine the existence of coverage and temperature regimes for which O/Rh(111) is ordered and CO oxidation rates are measurable.

## 2. Experimental

The apparatus, described elsewhere [3,10,12], consists of a three molecular-beam source, a UHV chamber with rotatable quadrupole mass spectrometer, and the controlling computer system. We note here that the center beam was used to produce a room temperature 63 meV He beam, and that the side beams were used to dose the Rh(111) crystal with  $O_2$ . The chamber pressure rise due to the He beam was typically  $3\text{--}9 \times 10^{-9}$  Torr, and the straight-through (unscattered) beam has a full-width at half-maximum (FWHM) of  $1^\circ$ . The computer system was used to control shutter timing, temperature, and mass spectrometer rotation as well as to collect titration, TPD, reflectivity, and diffraction data. The surface temperature was maintained and measured to within 0.1 K with a Eurotherm temperature controller. The surface was heated resistively and cooled via a liquid nitrogen cold finger. Beam fluxes were measured in a straightforward manner using enclosed Bayert–Alpert gauges which had entrance apertures aligned along the molecular beam path to intercept the incident molecular beams within the UHV chamber. Incident beam intensity was determined with this arrangement by noting the steady state pressure rise indicated by the gauge when the beam was on; under steady-state conditions the flux emanating out of the apertured gauge equals the incident flux, and hence the beam flux can be directly determined. The maximum flux for CO,  $N_2$ , and  $O_2$  was  $1.0 \pm 0.2$  ML/s ( $1 \text{ ML/s} = 1.6 \times 10^{15}$  molecules/cm $^2 \cdot$  s).

## 3. Results and discussion

### 3.1. He diffraction

#### 3.1.1. 0.25 ML ( $2 \times 2$ )-O/Rh(111)

O/Rh(111) overlayer structures have been studied by many at low temperatures [13–22], but there is little data to show what happens when the Rh(111) surface is heated to CO oxidation reaction temperatures ( $T_s = 450\text{--}625$  K). There are two well known O/Rh(111) structures, the 0.25 ML ( $2 \times 2$ ) structure and the 0.50 ML ( $2 \times 2$ ) or mixed ( $2 \times 1$ ) structure. A variety of measurements have indicated that adsorbed O sits at three-fold hollow sites for both structures [18–21].

We created the 0.25 ML ( $2 \times 2$ ) structure on our Rh(111) surface by dosing the surface with a weak intensity ( $< 0.2$  ML/s) 88 meV  $O_2$  beam until a sharp diffraction peak was observed with a 63 meV  $45^\circ$  incident He beam at  $55^\circ$  for  $T_s = 350$  K. These diffraction measurements confirm the Rh–Rh spacing of 2.69 Å or the nearest O neighbor spacing of 5.37 Å for the ( $2 \times 2$ ) 0.25 ML O/Rh(111) overlayer. We note that, as the crystal is heated above  $T_s = 450$  K, the  $36^\circ$  and  $55^\circ$  peak intensities are attenuated, but even at 525 K, there are still diffraction peaks, evidence of ( $2 \times 2$ ) domains which persist at  $\theta_0 = 0.25$  ML up to CO oxidation temperatures.

#### 3.1.2. 0.50 ML O/Rh(111) overlayer

LEED studies have indicated the structure of the 0.50 ML O/Rh(111) overlayer is a ( $1 \times 2$ ) or a mixed ( $1 \times 2$ ) structure which appears as a ( $2 \times 2$ ) structure [13,20,22]. This overlayer is created by dosing with a 1 ML/s 88 meV  $O_2$  beam at  $T_s < 350$  K. At higher temperatures, excess O is deposited subsurface [15,23]. As shown in Fig. 1, sharp diffraction peaks for a 63 meV  $45^\circ$  incident He beam are visible at  $T_s = 125\text{--}350$  K. These peaks continue to attenuate until, at 600 K, no diffraction is visible, indicating that ordered ( $1 \times 2$ ) or ( $2 \times 2$ ) domains persist at  $\theta_0 = 0.50$  ML up to at least 550 K, which covers most of the range for CO oxidation temperatures.

We note here that the saturation value for  $T_s < 350$  K O/Rh(111) overlayer had been quoted in early work on this system as  $\theta_0(\text{sat}) = 0.83$  [14], and our

subsequent papers (as well as work from other groups) used this incorrect value [3,24]. The correct value of  $\theta_0(\text{sat}) = 0.50$  ML has been more recently confirmed by comparisons of XPS intensities of the known  $(2 \times 2)$  0.75 ML CO/Rh(111) and the known  $(\sqrt{3} \times \sqrt{3})$ -R30° S/Rh(111) overlayers to the saturated O/Rh(111) overlayer [22]. We confirmed this value by comparing the (flux density corrected) CO TPD intensity of the known 1/3 ML  $(\sqrt{3} \times \sqrt{3})$ -R30° CO/Rh(111) overlayer to the (flux density corrected) O<sub>2</sub> TPD intensity for the saturated O/Rh(111) overlayer. We also compared the CO<sub>2</sub> intensity (collected at several angles) from an O<sub>2</sub> titrated 1/3 ML  $(\sqrt{3} \times \sqrt{3})$ -R30° CO/Rh(111) overlayer to the CO<sub>2</sub> intensity of the CO titrated saturated O/Rh(111) overlayer. The comparison showed that  $\theta_0(\text{sat}) = 0.47 \pm 0.04$  ML.

### 3.1.3. Coverage dependent O / Rh(111)

By utilizing specular He scattering (see Section 3.2), we monitored  $\theta_0$  as we exposed the Rh(111) to various doses of O<sub>2</sub>. The 63 meV 45° incident He beam He diffraction curves for  $T_s = 225$  K (Fig. 2) indicate that  $(2 \times 2)$  domains will start to form at

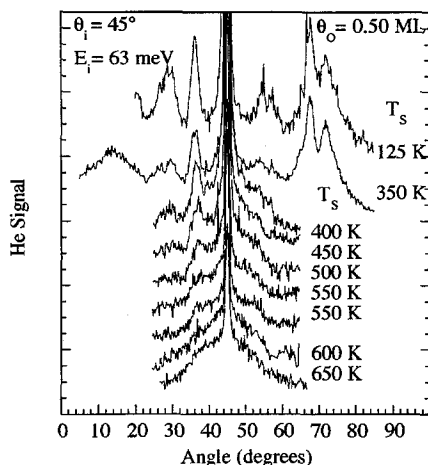


Fig. 1. He diffraction from 0.50 ML O/Rh(111). Shown are temperature dependent He diffraction plots for the well known (see text) 0.50 O overlayer on Rh(111). The incident He beam conditions (shown) along the  $\langle 11\bar{2} \rangle$  azimuth produce  $(\frac{1}{2}, \frac{1}{2})$  and  $(0, 0)$  diffraction peaks at 36° and 45° from normal, but the  $(\frac{1}{2}, \frac{1}{2})$  and  $(\bar{1}, \bar{1})$  peaks at 56° and 27°, respectively, are split. By following the attenuation of the  $(\frac{1}{2}, \frac{1}{2})$  peak at 36°, we note that domains of this overlayer's structure persist up to at least 550–600 K.

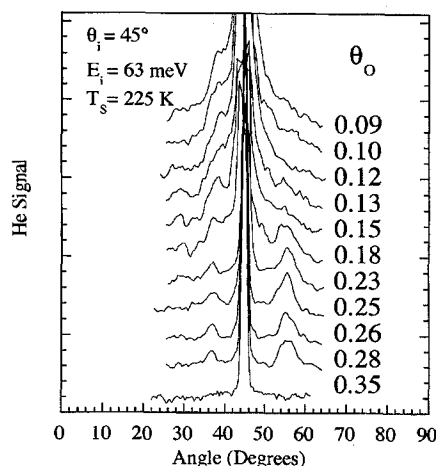


Fig. 2. Coverage dependent He diffraction from 225 K O/Rh(111). Shown are coverage dependent He diffraction plots for O overlayers along the  $\langle 11\bar{2} \rangle$  azimuth on 225 K Rh(111). The overlayers were heated to 400 K before each diffraction scan. The  $(2 \times 2)$  O domains are evident from the  $(\frac{1}{2}, \frac{1}{2})$  and  $(\frac{1}{2}, \frac{1}{2})$  diffraction peaks at 36° and 56°. Note the disappearance of any overlayer diffraction peaks at  $\theta_0 = 0.35$  ML, indicating the absence of any measurable ordered domains; there is no evidence of the domains which produce intense peaks at 36° for the well known ordered overlayers at  $\theta_0 = 0.25$  or 0.50 ML.

$\theta_0 \approx 0.15$  ML at  $T_s = 225$  K. By  $\theta_0 \approx 0.35$  ML, no diffraction peaks are visible, indicating that no  $(1 \times 2)$  or  $(2 \times 2)$  ordered domains exist at  $T_s = 225$  K in this coverage regime.

### 3.2. O coverage calibration for 63 meV He

Fig. 3 shows the attenuation in reflectivity of a 63 meV 45° incident specular He beam as the Rh(111) crystal is exposed to O<sub>2</sub> at  $T_s = 450$ –550 K. The measured  $I_{O_2}$  was  $0.10 \pm 0.02$  times the maximum beam flux ( $1.0 \pm 0.2$  ML/s), so  $I_O = 0.20 \pm 0.08$  ML/s. He reflectivity  $[I_{He}(\theta_0)/I_{He}(0)]$  is defined as the ratio of the specular He intensity at a given temperature and adsorbate coverage to the specular He intensity at the same given temperature with no adsorbate coverage. Except for the 450 K data at  $t > 10$  s, the lines are virtually identical, indicating a temperature independent relationship over this temperature regime between O exposure (i.e.  $\theta_0$ ), and He reflectivity. As indicated by the He diffraction measurements (see Figs. 1 and 2), the deviation for the 450 K data at higher coverages (i.e. longer

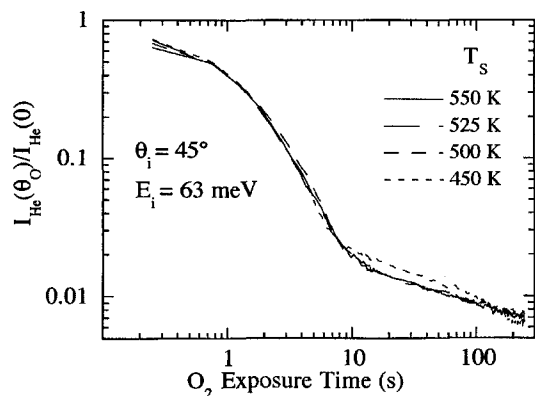


Fig. 3. He reflectivity versus  $O_2$  exposure on 450–550 K Rh(111). Shown is the He reflectivity versus  $O_2$  exposure time for a  $0.10 \pm 0.02$  ML/s 88 meV  $O_2$  beam onto Rh(111) at 4 different surface temperatures: 450, 500, 525, and 550 K. Since  $O_2$  dissociates upon sticking to Rh(111),  $I_0 = 2I_{O_2}$ . Note that the reflectivities decrease at the same rate for all temperatures above 450 K, indicating that there is little temperature dependence in the relationship between O coverage and He reflectivity at these temperatures. The slight deviation for the 450 K line is probably due to added specular intensity from diffraction from an ordered O overlayer at higher coverages.

exposure times) is due to increased He diffraction from the O overlayer.

Since the He reflectivity attenuation is temperature independent over a wide range of the CO oxidation temperatures,  $T_s = 450$ –550 K, we can use a single calibration for the entire range, as long as we are careful to adjust our calibration at  $T_s$  near 450 K for diffraction at higher coverages. First we observed the adsorption isotherm for a low intensity ( $< 0.1$  ML/s)  $O_2$  beam by titrating adsorbed O off with CO (as  $CO_2$ ) and determining the  $CO_2$  intensity as a function of exposure time (Fig. 4a). As explained above, the maximum O coverage is known to be 0.50 ML. Inserting this maximum value for oxygen coverage and the measured beam intensity ( $I_0 = 2I_{O_2} = 0.10 \pm 0.08$  ML/s) into the expression for second order adsorption kinetics given in the Fig. 4a inset, we can extract the sticking coefficient from the experimentally determined value of  $SI_0 = 0.0456$  ML/s; the sticking coefficient so determined is  $S = 0.046 \pm 0.037$  for  $O_2$  on 525 K Rh(111). Next we measured the He reflectivity as we exposed the clean surface again to the same low intensity  $O_2$  beam (Fig. 4c).

As shown in Fig. 4b,  $O_2$  adsorption appears to be second order for the 88 meV incident  $O_2$  beam (linear for  $2\theta_0/(1-2\theta_0)$ ), contrary to the Yates et al. [16] claim that  $O_2$  adsorption is first order (linear for  $\ln(\theta_0)$ ). Second order Langmuir adsorption indicates that two adjacent unoccupied sites are necessary for adsorption, while first order Langmuir adsorption indicates that adsorption occurs at single

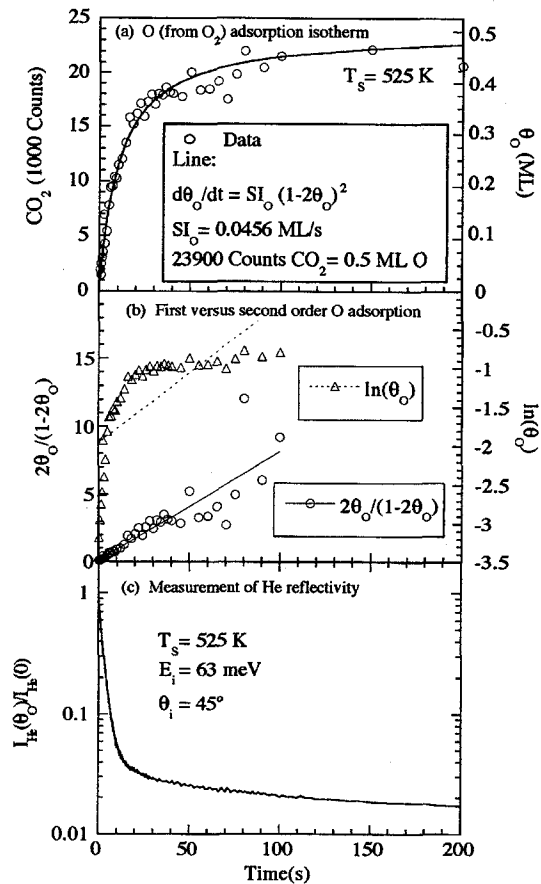


Fig. 4. He reflectivity and  $O_2$  adsorption isotherms for 63 meV He. Shown are the results of two experiments used to calibrate He reflectivity to O coverage. In the first experiment (panel (a)) a low intensity 88 meV  $O_2$  beam is used to deposit O on the Rh(111) surface, as determined by CO titration (see text). Panel (b) demonstrates that the resulting isotherm is best described by a second order Langmuir isotherm (see text). Best fit results of the second order Langmuir isotherm fit are shown in the box in panel (a). In the second experiment (panel (c)) the same low intensity 88 meV  $O_2$  beam deposits O on the surface, and the resulting decrease in He reflectivity for a  $45^\circ$  incident 63 meV He beam is monitored.

unoccupied sites. There are several differences between the measurements in Ref. [16] and our measurements which could affect the shape of the adsorption curve.  $\theta_{\text{O}}$  in Ref. [16] was measured using Auger spectroscopic ratios of O to Rh peak to peak amplitudes, which were shown in Ref. [15] *not* to correspond well with the  $\text{O}_2$  desorption intensity measurements of  $\theta_{\text{O}}$  (see figure 2 in Ref. [15]). We note that the  $\text{O}_2$  adsorption measurements in Ref. [16] were made by exposing the Rh(111) crystal to a background pressure of  $\text{O}_2$  on a 335 K Rh(111) surface. The mean  $\text{O}_2$  translational energy in Ref. [16] is a much slower 43 meV with a much wider velocity spread, and therefore a different adsorption mechanism (i.e., precursor for slower versus direct for faster) could dominate adsorption. Another difference is that, at 335 K, there is significantly more ordering of O on Rh(111) than at 525 K (see Figs. 1 and 2 in this paper, figures 3–7 in Ref. [16], and Ref. [15]). From our data, we calculate a sticking coefficient of about 5% for  $\text{O}_2$  on 525 K Rh(111).

The combined results of the panels (a) and (c) in Fig. 4 were used to produce a calibration curve for 63 meV He from 525 K O/Rh(111) (Fig. 5, solid line). For  $\theta_{\text{O}} = 0$ –0.21 ML (monolayers), the relationship between reflectivity and  $\theta_{\text{O}}$  is very well described by the Comsa–Poelsema model [11] for randomly distributed, repulsively interacting adsorbates ( $m > 1$ ) on a lattice (Fig. 5, longer spaced dashed line):

$$\frac{I_{\text{He}}(\theta_{\text{O}}, T_{\text{S}})}{I_{\text{He}}(0, T_{\text{S}})} = (1 - m\theta_{\text{O}}) \frac{\Sigma_{\text{He-O}}\eta}{m}, \quad (1)$$

where the left side of Eq. (1) is the He reflectivity at  $\theta_{\text{O}}$  and  $T_{\text{S}}$ ,  $\Sigma_{\text{He-O}} = 62 \pm 2 \text{ \AA}^2$  is a fit parameter which represents the He attenuation cross section for 63 meV He scattered from O/Rh(111),  $\eta = 0.160 \text{ \AA}^{-2}$  is the known Rh atom density, and  $1/m = 0.53 \pm 0.08$  is a fit parameter which represents the maximum possible coverage for the system. The fact that  $1/m < 1$  indicates repulsive interactions between coadsorbed O atoms. We note here a previous error for  $\eta$  in Ref. [10], and thus for a 63 meV  $45^\circ$  incident He beam and CO/Rh(111), the correct  $\Sigma_{\text{He-CO}} = 120 \text{ \AA}^2$  (almost identical to the 63 meV  $40^\circ$  incident He beam attenuation cross section of  $123 \text{ \AA}^2$  for CO/Pt(111) [11]). We also note that  $m = 3.163$  for the 63 meV  $45^\circ$  incident He from

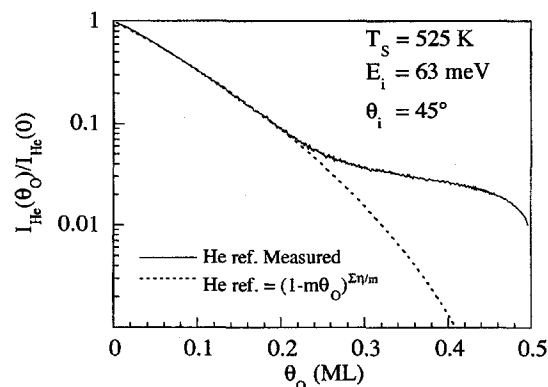


Fig. 5. O/Rh(111) coverage He reflectivity calibration for 63 meV He. The combined results of the experiments shown in Fig. 4 are used to produce a measured calibration curve (solid line) for He reflectivity as a function of  $\theta_{\text{O}}$  for a  $45^\circ$  incident 63 meV He beam. For  $\theta_{\text{O}} < 0.21$  ML, the relationship between reflectivity and  $\theta_{\text{O}}$  is well described by the Comsa–Poelsema model (Eq. (1)) for randomly distributed (i.e., disordered) adsorbates on a lattice with the following fitting parameters:  $\Sigma_{\text{He-O}} = 62 \pm 2 \text{ \AA}^2$  (cross section),  $\eta = 0.160 \text{ \AA}^{-2}$  (Rh atom density), and  $1/m = 0.53 \pm 0.08$ . The relationship at higher coverages could not be described by a simple model; this deviation from the Comsa–Poelsema model indicates that the overlayer has ordered domains at these higher coverages.

CO/Rh(111). The relationship between He reflectivity and  $\theta_{\text{O}}$  could not be described by a simple model for  $\theta_{\text{O}} > 0.21$  ML.

#### 4. Summary and conclusion

He scattering from the O/Rh(111) overlayer for  $T_{\text{S}} = 125$ –625 K and  $\theta_{\text{O}} = 0.0$ –0.50 ML indicates the existence of ordered regimes at high coverage and low temperatures, and disordered regimes at low coverages and high temperatures. For  $\theta_{\text{O}} < 0.21$  ML and  $T_{\text{S}} > 450$  K, the He reflectivity is described well by the Comsa–Poelsema model for repulsively interacting, disordered adsorbates, with a cross section for a 63 meV  $45^\circ$  incident He beam of  $62 \pm 2 \text{ \AA}^2$ . For  $0.21 \text{ ML} < \theta_{\text{O}} < 0.35 \text{ ML}$  and  $T_{\text{S}} < 525 \text{ K}$ , He diffraction from the O/Rh(111) overlayer indicates the existence of  $(2 \times 2)$  ordered domains. At  $\theta_{\text{O}} = 0.35 \text{ ML}$ , and  $T_{\text{S}} < 225 \text{ K}$ , there are no observed ordered domains. At the measured saturation value of 0.50 ML, a  $(2 \times 2)$  diffraction pattern is observed, probably due to rotated  $(1 \times 2)$  domains.

Kinetic measurements of O<sub>2</sub> adsorption for an 88 meV (680 K) O<sub>2</sub> beam indicate second order Langmuir adsorption of O<sub>2</sub> on Rh(111) at 525 K. From our data, we calculate a sticking coefficient of about 5% for O<sub>2</sub> on 525 K Rh(111). Since catalytic oxidation of CO on Rh occurs for  $T_s > 450$  K, our results are indicative of the coverage and temperature conditions at which CO oxidation occurs. With these results, we have successfully demonstrated the possibility and utility of utilizing concurrent molecular beam reactive scattering and He diffractive scattering to study model single crystal systems at catalytic coverages, gas temperatures, and surface temperatures.

### Acknowledgements

The authors wish to thank Dr. Kevin Gibson and Jennifer Colonell for their helpful suggestions. Acknowledgment is made to the donors of The Petroleum Research Fund, administered by the ACS, for partial support of this research. Additional support from the NSF Materials Research Science and Engineering Center at The University of Chicago is also gratefully acknowledged.

### References

- [1] M.P. D'Evelyn and R.J. Madix, Surf. Sci. Rep. 3 (1984) 413.
- [2] C.T. Campbell, G. Ertl, H. Kuipers and J. Segner, J. Chem. Phys. 73 (1980) 5862.
- [3] L.S. Brown and S.J. Sibener, J. Chem. Phys. 89 (1988) 1163.
- [4] S.B. Schwartz, L.D. Schmidt and G.B. Fisher, J. Phys. Chem. 90 (1986) 6194.
- [5] H.P. Bonzel and R. Ku, Surf. Sci. 33 (1972) 91.
- [6] H. Conrad, G. Ertl and J. Küppers, Surf. Sci. 76 (1978) 323.
- [7] C.T. Campbell, S.-K. Shui and J.M. White, J. Phys. Chem. 83 (1979) 2255.
- [8] C.T. Campbell, S.-K. Shui and J.M. White, Appl. Surf. Sci. 2 (1979) 382.
- [9] C.T. Campbell, S.-K. Shui and J.M. White, J. Vac. Sci. Technol. 16 (1979) 605.
- [10] K.A. Peterlinz, T.J. Curtiss and S.J. Sibener, J. Chem. Phys. 95 (1991) 6972.
- [11] B. Poelsema and G. Comsa, Scattering of Thermal Energy Atoms from Disordered Surface (Springer, New York, 1989).
- [12] K.D. Gibson and S.J. Sibener, J. Chem. Phys. 88 (1988) 791.
- [13] D.G. Castner, B.A. Sexton and G.A. Somorjai, Surf. Sci. 71 (1978) 519.
- [14] T.W. Root, L.D. Schmidt and G.B. Fisher, Surf. Sci. 134 (1983) 30.
- [15] P.A. Thiel, J.T. Yates, Jr. and W.H. Weinberg, Surf. Sci. 82 (1979) 22.
- [16] J.T. Yates, Jr., P.A. Thiel and W.H. Weinberg, Surf. Sci. 82 (1979) 45.
- [17] D.G. Castner and G.A. Somorjai, Appl. Surf. Sci. 6 (1980) 29.
- [18] P.C. Wong, K.C. Hui, M.Y. Zhou and K.A.R. Mitchell, Surf. Sci. 165 (1986) L21.
- [19] N. Winograd, P.H. Kobrin, G.A. Schick, J. Singh, J.P. Baxter and B.J. Garrison, Surf. Sci. 176 (1986) L817.
- [20] C.T. Reimann, M. El-Maazawi, K. Walz, B.J. Garrison, N. Winograd and D.M. Deaven, J. Chem. Phys. 90 (1989) 2027.
- [21] A.D. Logan, A.K. Datye and J.E. Houston, Surf. Sci. 245 (1991) 280.
- [22] X. Xu and C. Friend, J. Am. Chem. Soc. 113 (1991) 6779.
- [23] K.A. Peterlinz and S.J. Sibener, J. Phys. Chem. 99 (1995) 2817.
- [24] D.F. Padowitz, K.A. Peterlinz and S.J. Sibener, Langmuir 7 (1991) 2566.